09/287560

PCT/GB 99/03133

GB99/3133

EJU

PA 184953

THE UNITED STATES OF AMERICA

TO ALL TO WHOM THESE PRESENTS SHALL COME:

UNITED STATES DEPARTMENT OF COMMERCE

United States Patent and Trademark Office

December 13, 1999

THIS IS TO CERTIFY THAT ANNEXED HERETO IS A TRUE COPY FROM THE RECORDS OF THE UNITED STATES PATENT AND TRADEMARK OFFICE OF THOSE PAPERS OF THE BELOW IDENTIFIED PATENT APPLICATION THAT MET THE REQUIREMENTS TO BE GRANTED A FILING DATE UNDER 35 USC 111.

APPLICATION NUMBER: ***60/126,871***
FILING DATE: ***March 30, 1999***

PRIORITY DOCUMENT
SUBMITTED OR TRANSMITTED IN COMPLIANCE WITH RULE 17.1(a) OR (b)

By Authority of the
COMMISSIONER OF PATENTS AND TRADEMARKS

L. Edelen

L. EDELEN
Certifying Officer

EXPRESS MAIL LABEL NO. EL122360330US

Aprov

PTO/SB/16(11-95)Approved for use through 01/31/98 OMB0651-0037
Patent and Trademark Office, U.S. DEPARTMENT OF COMMERCE

PROVISIONAL APPLICATION FOR PATENT COVER SHEET

This is a request for filing a PROVISIONAL APPLICATION FOR PATENT under 37 CFR 1.53(b)(2).

Docket Number		Type a plus sign (+) inside this box =>	+

INVENTOR(S) / APPLICANT(S)

LAST NAME	FIRST NAME	MIDDLE INITIAL	RESIDENCE (CITY AND EITHER STATE OR FOREIGN COUNTRY)
Dobson	Christopher	M.	Oxford, England
Sunde	Margaret	n.m.i	Oxford, England
Guijarro	Joseba	I.	Oxford, England

TITLE OF THE INVENTION (230 characters max)

FIBRILS

CORRESPONDENCE ADDRESS

Carl R. Schwartz, Esq.
Quarles & Brady LLP
411 E. Wisconsin Ave
Milwaukee WI 53202-4497

STATE	Wisconsin	ZIP CODE	53202	COUNTRY	U.S.A.

ENCLOSED APPLICATION PARTS (check all that apply)

X	Specification	Number of pages	28		Small Entity Statement
X	Drawing(s)	Number of sheets	7		Other (specify)

METHOD OF PAYMENT OF FILING FEES FOR THIS PROVISIONAL APPLICATION FOR PATENT (check one)

	A check of money order is enclosed to cover the provisional filing fees	PROVISIONAL FILING FEE AMOUNT($)	$150.00
X	The Commissioner is hereby authorized to charge filing fees and credit Deposit Account Number: 17-0055 plus any other needed fees		

The invention was made by an agency of the United States Government or under a contract with an agency of the United States Government.

[X] No
[ ] Yes, the name of the U.S. Government agency and the Government contract number are: _____

Respectfully submitted,

SIGNATURE _____ Date 3/30/99

TYPED or PRINTED NAME Carl R. Schwartz REGISTRATION NO. (if appropriate) 29,437

[ ] Additional inventors are being named on separately numbered sheets attached hereto MKE\4340778

USE ONLY FOR FILING A PROVISIONAL APPLICATION FOR PATENT

FIBRILS

The present invention relates to amyloid fibrils, processes for their preparation and their use. The invention in particular relates to both naturally occurring amyloid fibrils and non-naturally occurring amyloid fibrils comprising a protein, their preparation and their use, for example, as a slow-release form of pharmaceutically active proteins, or in the delivery of pharmaceutically active compounds, electronics or catalysis.

The amyloidoses are a group of protein misfolding disorders characterised by the accumulation of insoluble fibrillar protein material in extracellular spaces. The deposition of normally soluble proteins in this insoluble form is believed to lead to tissue malfunction and cell death. A number of different proteins and polypeptides have been identified in amyloid deposits to date. These include the Aβ peptide in Alzheimer's disease, the prion protein in the transmissible spongiform encephalopathies, the islet-associated polypeptide in type II diabetes, and other variant, truncated, or misprocessed proteins in the systemic amyloidoses (S.Y. Tan and M.B. Pepys (1994) *Histopathology* **25**, 403-414 and J.W. Kelly (1996) *Curr. Op. Struct. Biol.* **6**, 11-17).

Proteins known to form amyloid fibrils *in vivo*

appear to have no obvious sequence or structural similarities, and where the soluble folds of the amyloidogenic precursors are known they span the range of secondary, tertiary, and quaternary structural elements. In spite of this diversity, there is a body of evidence that indicates that all amyloid fibrils are long, straight and unbranching, with a diameter of from 7 to 12 nm, and they all exhibit a cross-β diffraction pattern. The protein molecules constitute individual or multiple beta-strands oriented perpendicular to the long axis of the fibril and forming long beta-sheets that propagate in the direction of the fibril twisting around each other.

The mechanism by which amyloidogenic proteins undergo the conversion from a soluble globular form to the cross-β conformation displayed by the disease-associated fibrils has not yet been elucidated. Nevertheless, the conformational reorganization associated with amyloid formation is well documented (J.W. Kelly (1997) *Structure* 5, 595-600. Studies of some of the amyloidogenic variants of transthyretin, lysozyme and the Ig light chain have investigated the process of conformational change that leads to amyloid deposition. Amyloid formation for the latter three proteins appears to start from partially structured forms of the proteins.

The present invention concerns naturally occurring amyloid fibrils, which to date have been associated with

disease, and non-naturally occurring amyloid fibrils comprising a protein which may have a variety of useful applications. The fibrils may be used, for example, as a slow-release form of pharmaceutically active proteins, or in the delivery of pharmaceutically active compounds, electronics or catalysis.

In a first aspect, the present invention provides amyloid fibrils substantially free of other protein.

In one embodiment the fibril is an amyloid fibril substantially free of other protein other than an amyloid fibril formed from an SH3 domain of a p85α subunit of bovine phosphatidylinositol 3-kinase at pH 2.0.

In a further embodiment the fibril is an amyloid fibril substantially free of other protein other than an amyloid fibril formed from an SH3 domain of a p85α subunit of bovine phosphatidylinositol 3-kinase.

The amyloid fibril may be naturally or non-naturally occurring. The naturally occurring amyloid fibrils of the present invention include, for example a fibril of the Aβ peptide associated with Alzheimer's disease, the prion protein associated with the transmissible spongiform encephalopathies, the islet-associated polypeptide associated with type II diabetes, transthyretin and fragments thereof associated with senile systemic amyloidosis, transthyretin variants and fragments thereof associated with familial amyloidotic polyneuropathy or

other variant or truncated or misprocessed proteins associated with systemic amyloidoses.

In a second aspect the present invention provides a non-naturally occurring amyloid fibril comprising a protein.

In one embodiment the fibril is a non-naturally occurring amyloid fibril comprising a protein other than an amyloid fibril formed from an SH3 domain of a p85α subunit of bovine phosphatidylinositol 3-kinase at pH 2.0.

In another embodiment the fibril is a non-naturally occurring amyloid fibril comprising a protein other than an amyloid fibril formed from an SH3 domain of a p85α subunit of bovine phosphatidylinositol 3-kinase.

In a further embodiment the fibril is a non-naturally occurring amyloid fibril comprising an SH3 domain of a p85α subunit of bovine phosphatidylinositol 3-kinase and at least one protein selected from a derivative or amino acid variant of an SH3 domain of a p85α subunit of bovine phosphatidylinositol 3-kinase, human muscle acylphosphatase or a derivative or amino acid variant thereof and bovine insulin or a derivative or amino acid variant thereof.

By "protein", as used herein, is meant one or more proteins, protein fragments, polypeptides or peptides. The protein is any protein capable of forming fibrils and

may be a pharmaceutically active protein.

The fibrils of the present invention may comprise non-naturally occurring proteins. The proteins may be, for example, proteins which have been chemically modified such as proteins which have been glycosylated or proteins which comprise a modified amino acid residue, a pharmaceutically active compound, a metal or a functional group such as a thiol group which is capable of binding one or more reactants. The protein is, for example a derivative or amino acid variant of an SH3 domain (PI3-SH3) of a p85α subunit of bovine phosphatidylinositol 3-kinase, human muscle acylphosphatase or bovine insulin.

The fibrils of the present invention are typically long, straight and unbranching. The diameter of the fibrils is generally from 1 to 20 nm, preferably from 5 to 15 nm and more preferably from 7 to 12 nm. The diameter of the fibrils may be varied by selecting suitable proteins.

It is believed that some of the fibrils of the present invention may comprise a hollow core which may be useful in a variety of applications.

It has been found that the fibrils of the present invention may be obtained by preparing a solution comprising a protein, typically one or more single chain polypeptides, said solution being in a state so that nucleation of the protein and fibril growth will occur

over an acceptable time, and allowing nucleation and fibril growth to take place.

By "nucleation", as herein used, is meant the initiation of processes that lead to fibril formation. Fibril formation from a solution involves, successively, protein self-association, formation of aggregates and fibril growth. Thus, desirably, the initiation solution is on the verge of instability. Nucleation and growth are slow processes and conditions are normally chosen so that fibril formation occurs over a period of hours or days. It will be appreciated that if nucleation occurs too rapidly then this will often have an adverse affect on fibril formation.

Nucleation can be caused by a variety of means including variations in solvents, concentration, salt, ligands, temperature and pH, as discussed below.

The solution comprising a protein may comprise any solvent or mixture of solvents in which nucleation can occur. For example, the solution may comprise DMSO, dioxan and/or water. Preferably the solution is an aqueous solution.

One or more organic solvents which can promote nucleation and fibril growth may be incorporated into the solution. In the case of naturally occurring proteins conditions are typically chosen to denature at least partially the protein whilst retaining conditions in

which self-association can occur. The organic solvent is generally water-miscible and is preferably an alcohol. The alcohol is typically a C_{1-6} alkanol which may be substituted or unsubstituted for example by one or more halogen atoms, especially fluorine atoms. Examples include methanol, ethanol, propanol or butanol, or fluorinated alcohols such as trifluoroethanol or hexafluoroisopropanol. Preferably the alcohol is trifluoroethanol. The concentration of alcohol is typically from 5 to 40% v/v and preferably about 25% v/v.

The concentration of protein in the solution is not limited in any way but it must be such that nucleation can occur. Generally the concentration is from 0.1 mM to 10 mM. Preferably the concentration of protein is about 1mM.

The temperature of the solution is generally from 0°C to 100°C. Preferably the temperature is from 0°C to 70°C, more preferably from 0°C to 40°C and most preferably from 5°C to 30°C.

The pH of the solution is any pH suitable for nucleation. Preferably the solution is acidic and more preferably the pH of the solution is from 0.5 to 6.5.

The solution may be seeded with, for example, previously formed particles of protein.

The fibrils of the present invention are suitably isolated by centrifugation, filtration or evaporation of

solvent. The fibrils thus obtained may then be washed and dried.

The fibrils of the present invention may be formed from pharmaceutically active proteins such as insulin, calcitonin, angiostatin or fibrinogen. The fibrils may therefore be used as a slow release form of such proteins due to the low solubility of the fibrils *in vivo*.

Alternatively, the fibrils of the present invention may be used in the delivery of pharmaceutically active compounds. They may, for example, comprise a protein which has been chemically modified to incorporate a pharmaceutically active compound or a pharmaceutically active compound may, for example, be retained inside a fibril with a hollow core by hydrogen bonding. Pharmaceutically active compounds which may be delivered using the fibrils of the present invention include, for example, cancer drugs such as cis Pt, anti-biotics, anti-inflammatories and analgesics.

The fibrils of the present invention may comprise one or more functional groups capable of binding one or more reactants. The functional groups may occur naturally in the protein of the fibrils or be incorporated by chemical modification. Reactants may be brought together inside fibrils with a hollow core or on the outside of fibrils.

The fibrils of the present invention may be used in

the treatment of, for example, diabetes, blood clotting disorders, cancer and heart disease.

The fibrils of the present invention may comprise a metal, such as copper, silver or gold, and form wires which may be useful in electronics.

The present invention is further illustrated, merely by way of example, with reference to the Figures in which:

Figures 1(a) to 1(d) show negative stain electron microscopy images of SH3 amyloids, showing a range of morphologies similar to those observed with disease-related fibrils. Figure 1(e) shows a cryo EM image and (f) shows the diffraction pattern of the form seen in (d) with an obvious helical twist, which was used for 3D reconstruction. The layer line spacing is around 60 nm, the asymmetric unit of the double helix. The various ribbons and smooth fibrils were formed at pH 2 (a,b) and pH 2.66 (c). The helical fibres formed at pH 2 are seen by negative stain in (d) and cryo EM in (e).

Figure 2 shows class averages (a,e), reprojections of 3D reconstructions (b,f), 1D projections (c,g) and diffraction patterns of the reprojections (d,h) for the 58 and 61 nm long repeats, respectively. (In this figure only, the fibre axis is horizontal). A region in (a) showing a ~3 nm periodicity is enlarged and marked with lines. The good agreement between the input class

averages and the reprojections of the 3D maps (compare a to b and e to f), and also between the diffraction pattern of a single fibril and of reprojected maps (g,h), supports the validity of the reconstruction procedure. The line projection comparisons (c,g) show that the 3D maps fit the input images better when the 2.7 nm subunit repeat is used in the reconstruction procedure than if the fibre is treated as continuous helix.

Figure 3 shows 3D reconstructions and contoured density sections of the 61 nm (a,c) and the 58 nm form (b,d). The fibrils are shown as rendered surfaces in a and c, and as contoured density cross-sections in c and d. The two independent reconstructions are very similar, and both show four protofilaments winding around a hollow core, with protruding edge regions. The 2.7 nm subunit repeat is most pronounced on the edge structure.

Figure 4 shows modelling the polypeptide fold in the fibrils. Figure 4 (a) shows a cross-section of the fibre and Figure 4 (b) shows a side view of a single protofilament. β-sheets derived from the PI3-kinase SH3 structure have been fitted into the map, after opening the β sandwich fold and reorientating and strengthening the strands. The remaining regions of polypeptide sequence are shown as disconnected dots, to indicate the number of residues present but not the conformation. At the angle of view in (a), the upper right and lower left

profilaments curve inwards below the plane of view, making the quality of the fit less apparent. The side view in (b) shows that the β-sheets fit well into the density.

Figure 5A shows a far-UV circular dichroism spectra of muscle acylphosphatase acquired during a fibrillogenesis process. The first and last spectra reported in the figure were acquired after 3 and 600 minutes from the initiation of the reaction, respectively. The spectra show a slow two-state transition between two conformations containing significant amounts of α-helical and β-sheet structure, respectively. After 600 minutes the spectra did not change their shapes but underwent a progressive reduction of signal and a shift of the negative peak towards the higher wavelengths, as a result of the accumulation of protein aggregates of major size. Figure 5B shows an amide I region of the infra-red spectrum of muscle acylphosphatase. The two peaks at 1613 and 1685 cm^{-1} indicate a cross-β structure.

Figures 6A-C are electron micrographs showing the morphological development of the muscle acylphosphatase aggregate. Figure 6A shows an aggregate of granular aspect after 72 minutes from initiation of the reaction. Figure 6B shows short fibrils after 32 hours. Figure 6C shows amyloid fibrils after two weeks. The scale bar

represents a distance of 100 nm. Figure 6D shows an optical microscope photograph of a sample containing muscle acylphosphatase-derived aggregate obtained after two weeks of incubation. The arrows indicate the blots of green birefringence coming from regions of amyloid fibril.

The Examples which follow further illustrate the present invention with reference to the Figures.

Examples

Example 1

Microscopy and image classification

Samples of twisted fibrils of the PI3-kinase SH3 domain formed after several months incubation at pH 2 (J.I. Guijarro *et al* (1998) *Proc. Natl. Acad. Sci. USA.* 95, 4224-4228) were vitrified on holey carbon grids, and low electron dose images were recorded at 120 kV and 1.3-1.5 µm underfocus on a JOEL 1200 EX microscope with an Oxford Instruments cryotransfer stage at 30,000x. Films were digitised on a Leafscan 45 linear CCD scanner (Ilford Ltd, Cheshire, UK) at a spacing of 10µm, and interpolated to 0.67 nm/pixel for processing. Calculated diffraction patterns (Figure 1f) were obtained by straightening fibres with Phoelix software, but the axial resolution was severely limited in the pitch, which ranged from 54.5 to 66 nm. In order to avoid resolution

loss due to non-linear interpolation, digitised fibres were cut into individual repeats and treated as single particles. 890-cut-out repeats were iteratively aligned and sorted into classes by multivariate statistical analysis, using either Imagic or Spider. This allowed identification of classes of repeats that were naturally straight and had the same length.

3D Reconstruction

Two class averages of with low inter-image variance, containing 92 and 77 images (~20% of the data set), corresponding to a 58 and 61 nm repeat respectively, were selected for 3D reconstruction. The repeat length was determined by cross-correlation of the class averages with the excised cross-over region. The subunit repeat was clearly observable in axial 1D projections of the class averages after square root amplitude filtering (Figure 2c,g). The repeat was determined as approximately 2.7nm in both cases, and the value used was chosen to give an integral number of subunits in the 58 and 61 nm repeats (21 and 22 subunits respectively). 3D reconstructions were calculated by back projection, assuming either a continuous helix or the 27 nm subunit repeat. The overall features of protofilament packing and density cross section were unaffected by imposition of a subunit repeat, but the line projections (Figure 2c,g)

and diffraction patterns (Figure 2d,h) of the reprojected images gave a better match to the input data when the 27 nm repeat was imposed. The diffraction pattern of the reprojected helix gave excellent agreement with the original one from the straightened fibre, and showed strong intensity to 22 nm resolution in the equatorial (radial) direction (Figure 1f). Resolution tests by Fourier shell correlation and phase residual between cross sections of the two maps (Figure 3c,d) show agreement to 2.5 nm, but there is reliable information to 2.2 nm in the equatorial direction for each map. The absolute handedness is not determined by this method and is arbitrary. Other procedures have been used for correlation of the helical disorder based on cross-correlation and back projection. The 3D maps were examined with AVS (Advanced Visualisation System) and β-sheet fitting was done in O.

The native fold of the 84 residue SH3 domain of the p85α subunit of bovine PI3 kinase contains five β-strands arranged in a β-sandwich. At low pH, the protein partially unfolds and assembles into amyloid fibrils. The images in Figures 1a to 1d show a range of twisted and flat ribbons, and smooth and twisted tubular fibres. For structural analysis, a form with a pronounced helical twist was selected. Diffraction patterns (Figure 1f) calculated from cryo EM images (Figure 1e) contain layers

at spacings between 54.5 to 66 nm, the distance between helical cross-overs in the double-helical structure, ie. the length of the helical repeat.

The diffraction data show structure information to 2.2 nm resolution in the equatorial direction (perpendicular to the fibre axis), but the meridional pattern fades out around 15 nm due to variations in the helical pitch (angular disorder). To retrieve the structural information lost due to angular disorder, the digitised images of the fibrils were divided up into individual helical repeats. These repeats were aligned and sorted into classes according to their length. The class averages of a 28 and a 61 nm repeat are shown in Figure 2 a,e, along with reprojections of 3D maps calculated from these two repeats (2b,f), and their diffraction patterns (2d,h). A subunit repeat is visible in the class average (Figure 2a, expanded) and sometimes in the raw images (not shown). A subunit periodicity of 2.7± 0.3 nm projections of the class averages was determined(Figure 2c,g).

The two independent 3D maps, derived from the 58 and 61 nm repeats, reveal the same features (figure 3). The surface views and cross sections show two pairs of thin profilaments winding around a hollow core. Regions of weaker density form the extended edges that give the fibrils their characteristic twisting appearance. The

profilaments are about 4 nm part and 2 nm thick (Figure 3c,d), too thin to accommodate the native SH3 structure, whose minimum dimension is 3 nm. X-ray fibre diffraction of SH3 amyloid indicates an ordered core of cross-β structure with a 0.47 nm meridional and a 0.94 nm equatorial repeat defining the inter-strand and inter-sheet distances respectively. The 2 nm width can only fit two β-sheets, which must be orientated differently from those in the native fold to make all the strands perpendicular to the fibre axis. The twist between β-strands is also very restricted by the narrow dimension and ling pitch of the profilaments, giving flat sheets with an inter-strand angle of less that 2°.

A model in which the SH3 are reorganised to fit into the EM density is shown in Figure 4. The remaining short and long loops are the right size range and provide the contracts between adjacent profilaments and to give rise to diffuse density in the protruding edges of the structure. Consistent with the observation that fibres are seen to split into sub-fibrils, that individual polypeptide chains could contribute β-strands to each member of a pair of protofilaments. Since the axial repeat corresponds to 5 β-strands, it is possible that this is related to the 2- and 3-stranded sheets of the native fold by a rearrangement similar to a domain swapping mechanism. Non-covalent interactions would then

provide the bonds assembling the adjacent sub-fibrils into the double helical structure.

The structure determined here, in which the protofilaments are effectively continuous β-sheets, may provide a basic model for all amyloid fibres, irrespective of the chain length and native conformation of the component protein. Indeed, negative stain EM, atomic force microscopy and fibre diffraction of Aβ(1-40) fibrils suggest a very similar morphology with two sub-fibrils and 3-5 protofilaments. EM studies of *ex vivo* transthyretin fibrils indicate that these consist of four protofilaments of diameter 5-6 nm. The transthyretin protofilament core has been modelled, based on X-ray fibre diffraction data, as four β-sheets with a 15° twist between adjacent strands. The two-sheet protofilament model presented here could however be extended to a larger number of sheets for thicker protofilaments. At present there is no evidence to discriminate between twisted and flat β-sheets in the larger protofilament type, but the maps are not consistent with as twisted sheet configuration for the SH3 protofilaments since they are only 2 nm thick and have a very small overall twist. Although flat, untwisted β-sheets are unusual in the protein structure database, part of the β-helix of alkaline protease has such a structure.

The cryo-EM work provides 3D information on how a

polypeptide chain is assembled into amyloid fibrils. Polymerisation into fibrils appears to require at least partial unfolding of native proteins and does not appear to be restricted to proteins whose native fold contains β-sheets. Indeed, formation of fibrils from native sheets of proteins is frequently associated with a conversion from helical to sheet structure. Even in the case of the SH3 domain, where the native fold is largely β structure, the structure of the fibrils suggests that this must be substantially rearranged relative to that of the native protein.

Example 2

Example 2 (i)

Muscle acylphosphatase was purified as previously reported (A. Modesti *et al.* (1995) *Protein Express Purif.* 6, 799) and incubated at a concentration of 0.375 mg/ml (34 μM) in 25 % v/v trifluoroethanol (TFE), acetate buffer, pH 5.5 at 25 °C under constant stirring. Aliquots were withdrawn at regular time intervals for electron microscopy and spectroscopic analysis. Circular dichroism spectra were acquired directly by means of a Jasco J-720 spectropolarimeter and cuvettes of 1 mm path length. Electron micrographs were acquired by a JEM 1010 transmission electron microscope at 80 kV excitation voltage. A 3 μL sample of protein solution was placed and

dried for five minutes on a Formvar and carbon-coated grid. The sample was then stained with 3 µL 1 % phosphotungstic acid solution and observed at magnifications of 25-100k.

Example 2 (ii)

Infrared spectra were acquired using BaF_2 windows of 50 µm path length.

Example 2 (iii)

Thioflavin T and Congo Red assays were performed according to Le Vine III (H. Le Vine III (1995) *Amyloid: Int. J. Exp. Clin. Invest.* **2**, 1.)and Klunk (W. E. Klunk *et al.* (1989) *J. Histochem. Cytochem.* **37**, 1293), respectively. For Congo Red birefringence experiments aliquots of protein were air dried onto glass slides. The resulting films were stained with a saturated olution of Congo red and sodium chloride, corrected to pH 10.0 with 1 % sodium hydroxide. The stained slides were examined by an optical microscope between crossed polarizers.

There is increasing evidence that amyloids develop not directly from the native and functional conformation ~~of the protein, but from an amyloidogenic precursor~~ bearing scant resemblance with the conformation of the native protein and identifiable in a denatured conformation containing a certain level of residual

structure. This conformation is often referred to as amyloidogenic intermediate. Muscle acylphosphatase is a protein that adopts, under physiological conditions, a well-defined fold, the stability of which is close to the average value for proteins of this size. Studies performed using trifluoroethanol (TFE) have revealed that muscle acylphosphatase is denatured at concentrations of TFE higher than 20-22% v/v. The denaturation of muscle acylphosphatase by TFE allows the maintenance of native α-helical structure of the protein and is accompanied by a virtual disruption of the hydrophobic core and by the concomitant formation of non-native α-helical structure. Further addition of TFE causes the accumulation of extra α-helical structure and the destabilisation of putative hydrophobic interactions that might be present under the lower alcohol concentrations. Therefore, an aqueous solution containing 25 % v/v TFE, the lowest alcohol concentration at which the native protein is virtually absent, was chosen for fibril formation.

The sequence of events after mixing was probed by a variety of techniques including far-UV circular dichroism (CD), tryptophane intrinsic fluorescence, Congo Red and Thioflavin T binding, electron microscopy and Congo Red birefringence. Following the rapid denaturation of the protein, occurring on a time-scale of seconds, far-UV CD analysis revealed the presence of a slow transition,

completed within 2-3 hours, from a conformation rich in α-helical structure to another containing a considerable content of β-sheet structure (Figure 5A). Far-UV CD spectra were acquired at regular time intervals over this period. The first CD spectrum is typical of a conformation rich in α-helical structure with two negative peaks centred at 208 and 222 nm. This spectrum changes gradually to a β-sheet spectrum with a single negative peak around 216 nm (Figure 5A) The presence of two isodichronic points at 210 and 225 nm suggests that such α/β transition consists of a two-state process. That such β-sheet structure derives from the intermolecular hydrogen bonding established within a protein aggregate is suggested by the two bands at 1685 and 1613 cm^{-1} in the amide region of the infra-red spectrum (Figure 5A) and by the electron micrographs revealing the presence of protein aggregates of granular aspect from samples recovered at this stage of the aggregation process (Figure 6A).

After a period of *ca.* 32 hours the electron micrographs revealed the presence of short filaments, indicating that a fibrillar protein aggregate had grown to a significant extent. After two weeks the fibrillar material was more evident. The fibrils revealed by the electron micrographs were long, unbranched and 8.5nm in width, whereas very short filaments or other protein

aggregates of granular aspect were no longer present. A series of optical tests were performed to investigate further the amyloid nature of this fibrillar material. A three fold increase of the 482 nm fluorescence (excitation 440 nm) of the dye Thioflavin T was observed as a consequence of the addition of the protein aggregate, a result expected for amyloids. In addition, the protein aggregate produced a red-shift of the maximum light absorption of the dye Congo Red. The subtraction of the absorption spectra of the aggregate alone and Congo red dye alone from the spectrum containing both the aggregate and the Congo Red dye produces a spectrum, with a maximum intensity at 540 nm. These two findings are also indicative of the presence of amyloid fibrils. Finally, the addition of Congo Red to a sample with muscle acylphosphatase-derived fibrils produced the characteristic green birefringence under cross-polarised light (Figure 6D). The development of green birefringence is highly diagnostic for the presence of amyloid fibrils. In summary, the muscle-acylphosphatase responded positively to all diagnostic tests for the presence of amyloid fibrils.

Recently, amphipathic compounds such as phospholipids have been suggested to facilitate the elongation of the fibrils. The formation of amyloid fibrils by fluoroalcohols like TFE supports this

suggestion that such amphipathic compounds normally present in biologic systems might act as a medium for the growth of amyloid fibrils *in vivo*.

Concentrations of TFE lower than 20 % or higher than 35 % did not lead to fibril formation. This may be because the fibrillogenesis process is hindered by the presence of the native conformation of the protein at low TFE concentrations or by the presence of denatured states too rich in α-helical structure at high concentrations of TFE. These may reduce the concentration of the amyloidogenic precursor acting therefore as kinetic traps for the process of fibril formation. Very high protein concentrations may also constitute an obstacle to the process of the fibrillogenesis process. When incubated at concentrations higher than 3 mg/ml muscle acylphosphatase led to the rapid and irreversible formation of a gel-like precipitate that electron microscopy revealed to be an amorphous protein aggregate. Amyloidogenesis, like crystallogenesis, is a process in which the protein molecules self-assemble to form ordered structures. High protein concentrations may favour the concentrations of molecules and accelerate any aggregation process. Under such conditions, however, there may not be sufficient time for formation of ordered and repetitive conformations.

CLAIMS

1. An amyloid fibril substantially free of other protein.

2. A fibril according to claim 1 which is a naturally occurring amyloid fibril.

3. A fibril according to claim 2 which comprises the Aβ peptide associated with Alzheimer's disease, the prion protein associated with the transmissible spongiform encephalopathies, the islet-associated polypeptide associated with type II diabetes, transthyretin and fragments thereof associated with senile systemic amyloidosis, transthyretin variants and fragments thereof associated with familial amyloidotic polyneuropathy or other variant, truncated, or misprocessed proteins associated with the systemic amyloidoses.

4. A non-naturally occurring amyloid fibril comprising a protein.

5. A fibril according to claim 4 wherein the protein is a non-naturally occurring protein.

6. A fibril according to claim 4 wherein the protein is selected from an SH3 domain (PI3-SH3) of a p85α subunit of bovine phosphatidylinositol 3-kinase or a derivative or amino acid variant thereof, human muscle acylphosphatase and bovine insulin.

7. A non-naturally occurring amyloid fibril comprising an SH3 domain (PI3-SH3) of a p85α subunit of bovine phosphatidylinositol 3-kinase and at least one protein selected from human muscle acylphosphatase, bovine insulin and the proteins as defined in claim 6.

8. A fibril according to claim 4 which further comprises a pharmaceutically active compound.

9. A fibril according to claim 4 which further comprises a metal.

10. A fibril according to claim 4 which further comprises a metal selected from copper, silver or gold.

11. A fibril according to claim 4 which further comprises one or more functional groups capable of binding one or more reactants.

12. A fibril according to claim 4 wherein the diameter of the fibril is from 1 to 20 nm.

13. A fibril according to claim 4 wherein the diameter of the fibril is from 5 to 15 nm.

14. A fibril according to claim 4 wherein the diameter of the fibril is from 7 to 12 nm.

15. A process for preparing an amyloid fibril which process comprises preparing a solution comprising a protein, said solution being in a state so that nucleation and fibril growth will occur over an acceptable time, and allowing nucleation and fibril growth to take place.

16. A process according to claim 15 wherein the solution further comprises an alcohol.

17. A process according to claim 15 wherein the solution further comprises an alcohol selected from methanol, ethanol, propanol, butanol, trifluoroethanol and hexafluoroisopropanol.

18. A process according to claim 15 wherein the concentration of protein in the solution is from 0.1

mM to 10 mM.

19. A process according to claim 15 wherein the temperature of the solution is from 0°C to 100°C.

20. A process according to claim 15 wherein the solution is acidic.

21. A process according to claim 15 wherein the pH of the solution is from 0.5 to 6.5.

22. A process according to claim 15 wherein the solution is seeded with previously formed particles of protein.

23. Use of a fibril according to claim 4 in electronics or catalysis.

24. A method of treating a human or animal, which method comprises administering thereto a non-toxic and effective amount of a fibril as claimed in claim 4.

25. A method according to claim 24 wherein the human or animal is suffering from or susceptible to diabetes, blood clotting disorders, cancer and heart disease.

ABSTRACT

FIBRILS

An amyloid fibril substantially free of other protein.

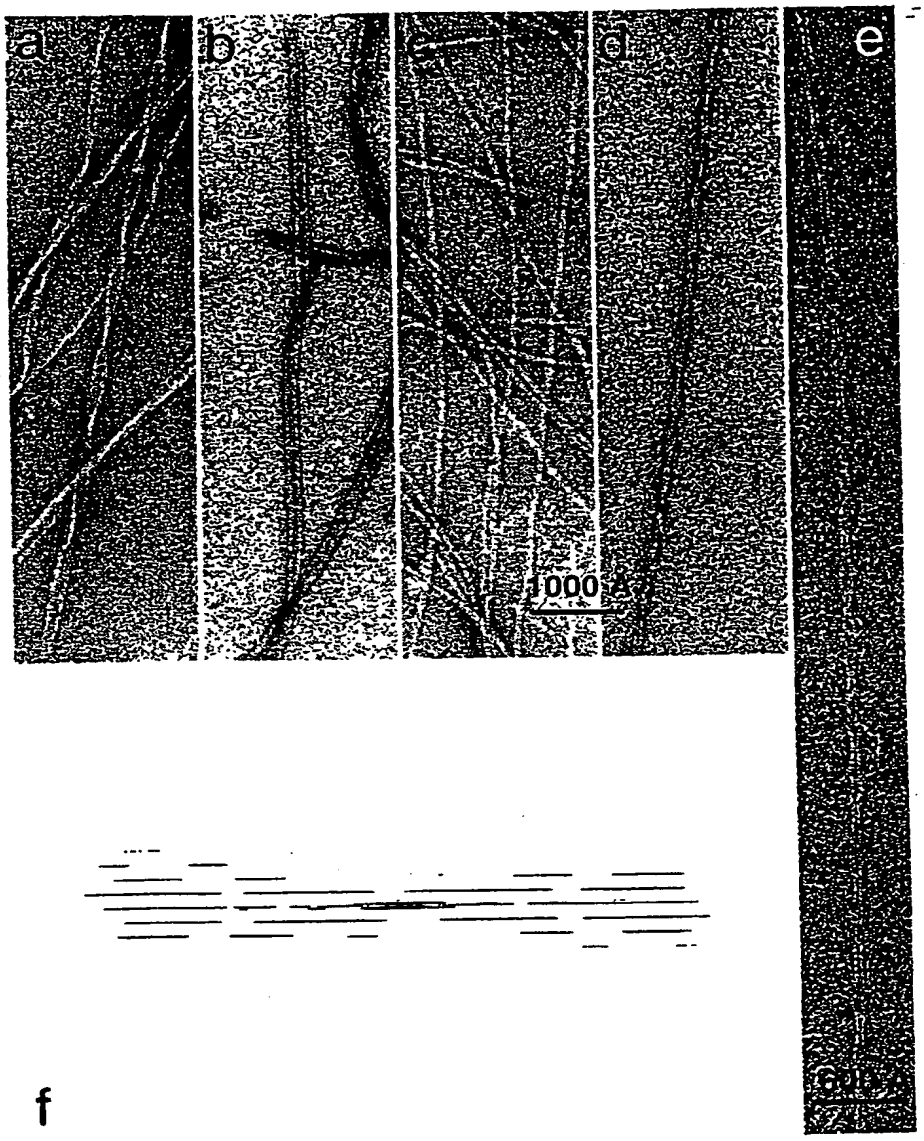

Figure 1

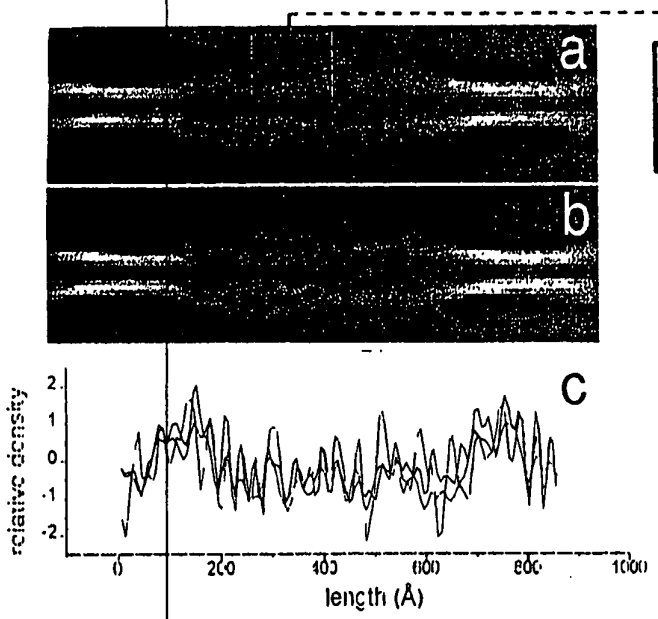
a
b
c
relative density
2
1
0
-1
-2
0
200
400
600
800
1000
length (Å)

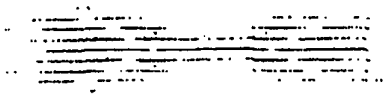

d

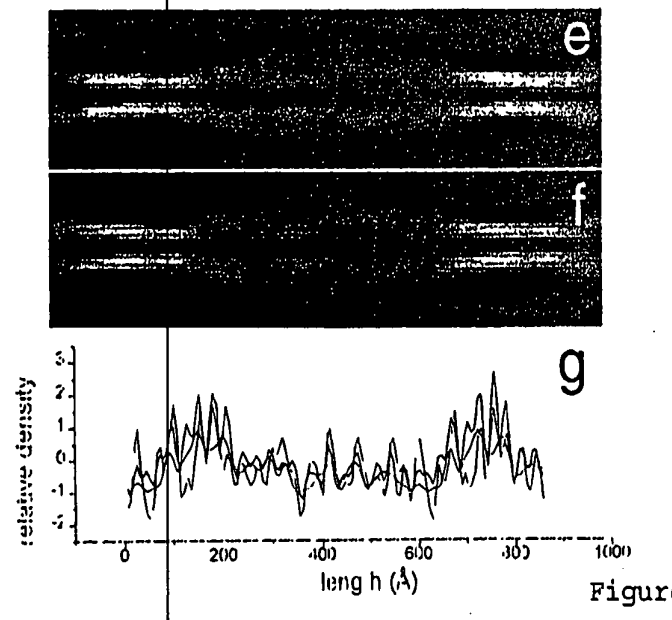
e
f
g
relative density
3
2
1
0
-1
-2
0
200
400
600
800
1000
leng h (Å)

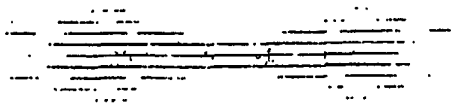

h

Figure 2

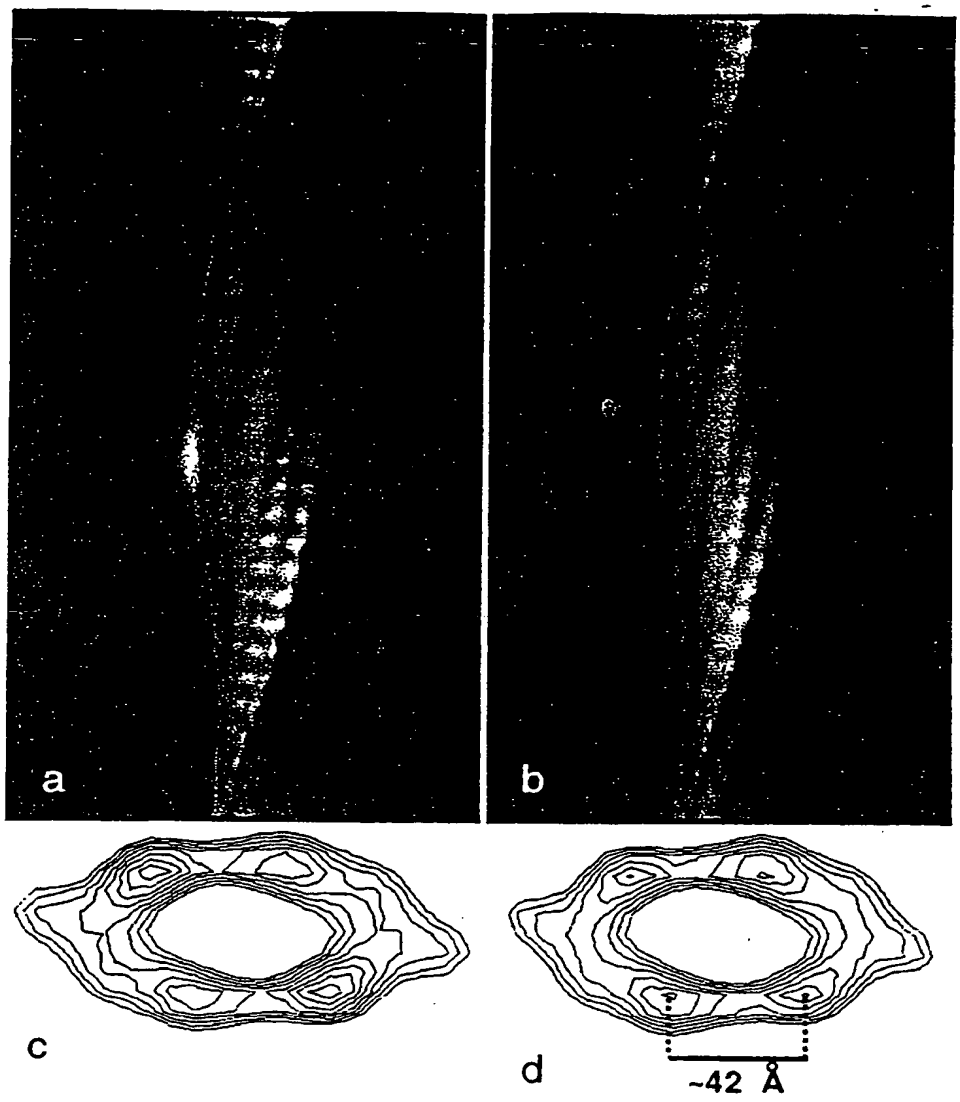

Figure 3

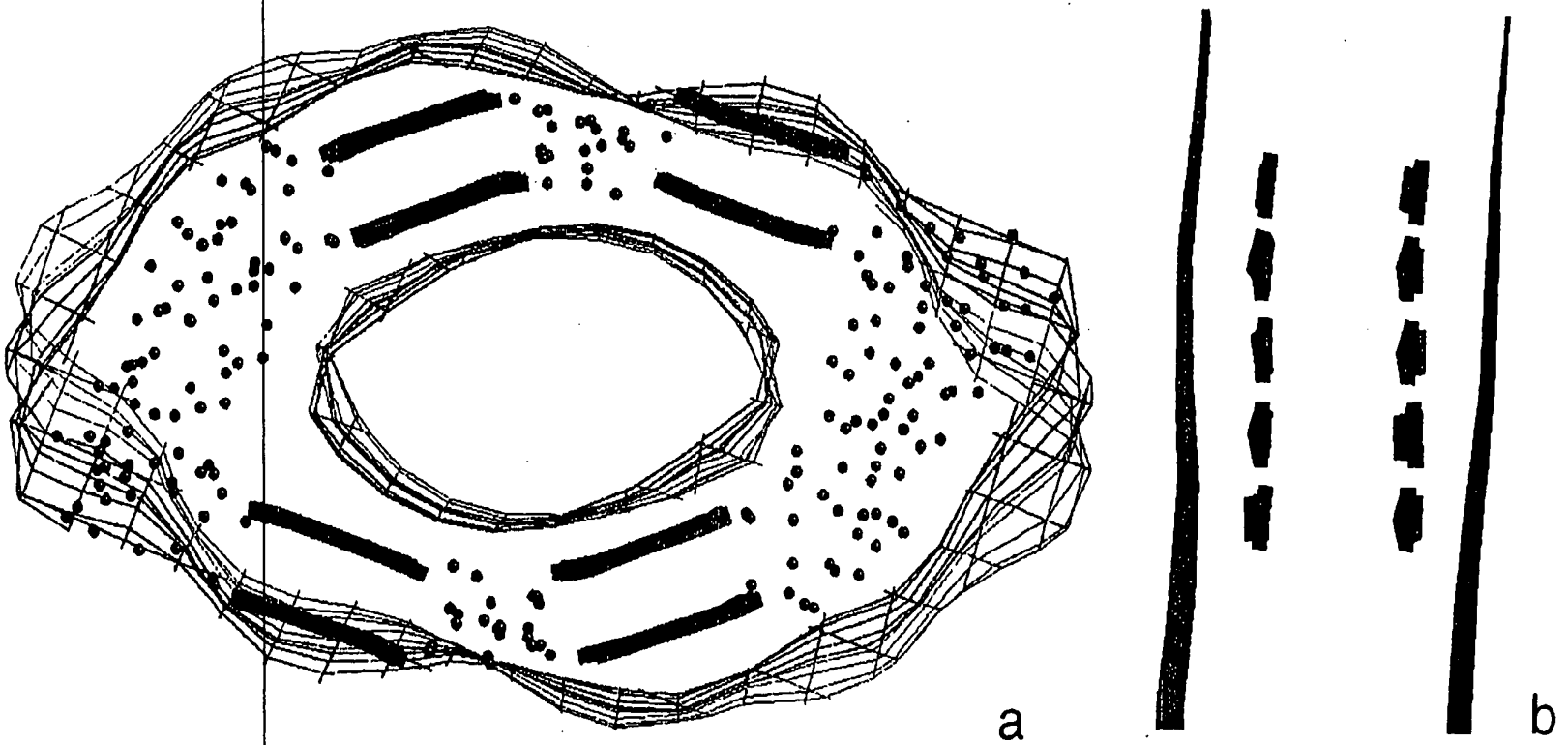

Figure 4

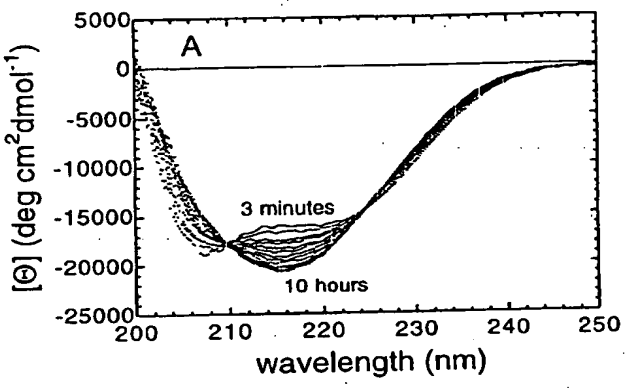
A
5000
0
-5000
-10000
-15000
-20000
-25000
[Θ] (deg cm²dmol⁻¹)
3 minutes
10 hours
200
210
220
230
240
250
wavelength (nm)

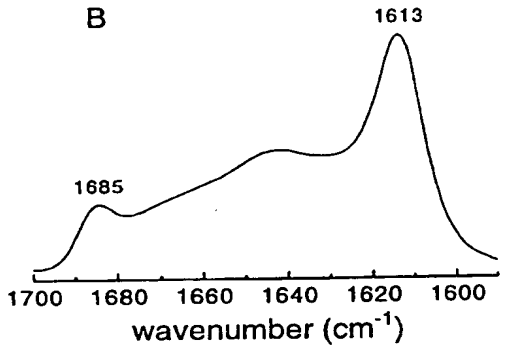
B
1613
1685
1700
1680
1660
1640
1620
1600
wavenumber (cm⁻¹)

Figure 5

Figure 6A

Figure 6B

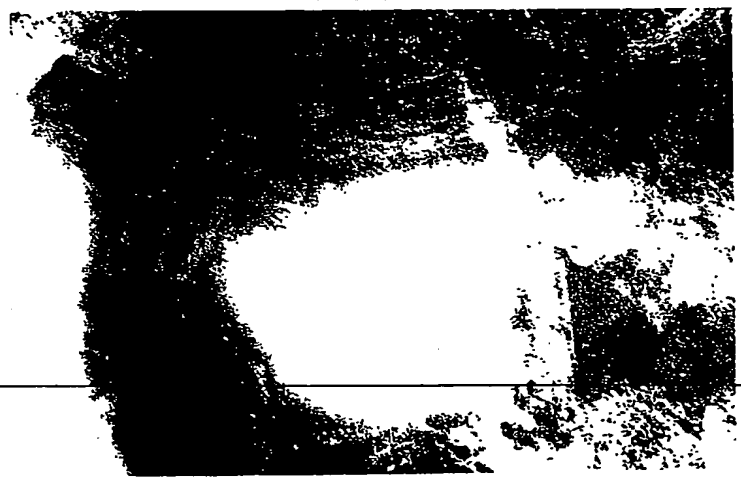

Figure 6C

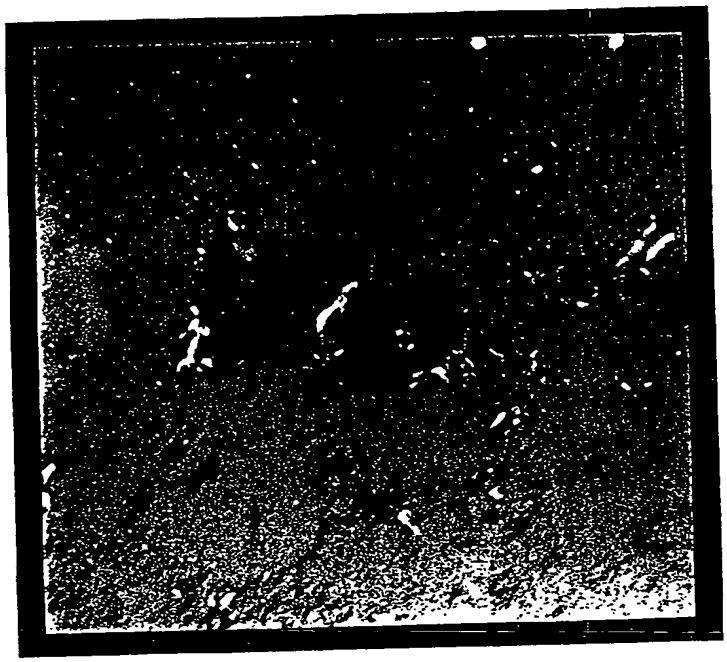

Figure 6D